Moroccan Journal of Chemistry
ISSN : 2351-812X

Mor. J. Chem., 2024, Volume 12, Issue 2, Page 776-798
https://revues.imist.ma/index.php/morjchem
https://doi.org/10.48317/IMIST.PRSM/morjchem-v12i2.46845

Molecular Docking and ADMET Prediction of Compounds from *Piper longum* L. Detected by GC-MS Analysis in Diabetes Management

Ram Lal Swagat Shrestha[1], Ritu Panta[1], Binita Maharjan[1], Timila Shrestha[1], Samjhana Bharati[1], Sujan Dhital[1], Prabhat Neupane[1], Nirmal Parajuli[1], Bishnu Prasad Marasini[2*], and Jhashanath Adhikari Subin[3*]

[1]Department of Chemistry, Amrit Campus, Tribhuvan University, Lainchaur, Kathmandu 44600, Nepal
[2]Nepal Health Research Council, Ramshah path, Kathmandu 44600, Nepal
[3]Bioinformatics and Cheminformatics Division, Scientific Research and Training Nepal P. Ltd., Bhaktapur 44800, Nepal
**For Corresponding author: Email address: subinadhikari2018@gmail.com / bishnu.marasini@gmail.com*

Received *13 Feb 2024,*
Revised *03 Mar 2024,*
Accepted *05 Mar 2024*

Citation*: Shrestha R. L. S., Panta R., Maharjan B., Shrestha T., Bharati S., Dhital S., Neupane P., Parajuli N., Marasini B. P., Adhikari Subin J. (2024) Molecular Docking and ADMET Prediction of Compounds from Piper longum L. Detected by GC-MS Analysis in Diabetes Management, Mor. J. Chem., 12(2), 776-798*

Abstract: Medicinal plants have been utilized for therapeutics against various diseases since ancient times. This study focuses on identifying bioactive compounds present in the fruit of plant *Piper longum* L. through GC-MS analysis. The molecular level computational exploration of its phytocompounds against diabetes through molecular docking and ADMET prediction were carried out. The results showed the presence of 33 different chemical components and the molecular docking calculation revealed that 5,6-dihydroergosterol, β-sitosterol, and piperine demonstrated better binding affinities of -9.7 kcal/mol, -9.5 kcal/mol, and -7.9 kcal/mol, respectively with α-amylase (PDB ID: 2QV4) and -9.1 kcal/mol, -9.4 kcal/mol and -8.1 kcal/mol respectively with α-glucosidase (PDB ID: 5ZCC). Most of the protein-ligand adducts exhibited significant binding of ligands with the receptor protein stronger than that of the reference drugs (miglitol, voglibose, and metformin). Moreover, the ADMET predictions (drug likeness and toxicity) suggested that the compounds were comparable with those of the reference drugs. These phytochemicals, specially 5,6-dihydroergosterol may be considered promising candidates for addressing diabetes due to their significant interferance with the normal functioning of α-amylase and α-glucosidase enzymes. The study recommends additional *in vitro* and *in vivo* experiments to validate the preliminary results.

Keywords: *Enzyme inhibition, Phytocompounds, Molecular docking, Scoring function, Solvent extraction*

1. Introduction

Natural compounds are biologically active compounds having a broad range of applications (Coman *et al*., 2012) originating from a variety of sources, including fungi, marine organisms, bacteria, and plants (Grenda *et al*., 2023). Such phytocomponents are extensively employed as active constituents in conventional and contemporary medicine to treat numerous diseases (Chintoju *et al*.,

2015). The presence of bioactive compounds like phenolic, tannins, alkaloids, flavonoids, glycosides, and terpenoids is the main reason behind the therapeutic value of the plants (Carsono *et al*., 2022; Duraipandiyan *et al*., 2006).

Piper longum L. (long pepper), is a flowering vine of the piperaceae family (Kumar *et al*., 2011). It is a dioecious, aromatic, trailing plant with perennial woody roots and jointed stems that grows in warm climates (Babu *et al*., 1976). *P. longum* exhibits as an essential candidate against cancer, diabetes, depression, and inflammation (Kaushik *et al*., 2012; Khushbu *et al*., 2011; Li *et al*., 2022). The fruit of *P. longum* consists of a large number of phytocompounds, with the most abundant being piperine, followed by methyl piperine, pipernonaline, asarinine, piperundecalidine, piperettine, piperlonguminine, piperlongumine, pipercide, and piperderidine (Priyadarshi *et al*., 2018; Scott *et al*., 2008).

Diabetes mellitus is a metabolic disorder, characterized by hyperglycemia, accountable for affecting millions of people worldwide and is considered one of the crucial health problems of the 21st century (Tolmie *et al*., 2021; Khandan *et al*., 2022). The α-amylase and α-glucosidase convert the dietary carbohydrates into simple monosaccharides which are absorbed and enter the bloodstream resulting hyperglycemia (Haddou *et al*., 2024; Magaña-Barajas *et al*., 2021). Thus, blocking the action of these enzymes can decrease carbohydrate metabolism, postpone glucose absorption, and ultimately lower blood sugar levels (Kajaria, 2013). The inhibition of α-amylase and α-glucosidase by inhibitors is one of the scientific approaches to manage type II diabetes. Inhibitors of α-amylase and α-glucosidase like miglitol, acarbose, and voglibose are considered as best medications. Still, they possess several side effects such as diarrhea, flatulence, bloating, and abdominal pain (Neupane *et al*., 2023). Therefore, there is an inclination towards the use of phytochemicals as potential therapeutic for diabetes treatment due to their fewer side effects and more effectiveness (Teoh & Das, 2018). *P. longum* was found highly effective in treating diabetes as a natural source (Kumar *et al*., 2013; Nabi *et al*., 2013), and their usage in ayurvedic medicine for diabetic management traces back to ancient times (Gaikwad *et al*., 2014). Due to its efficiency and cost-effectiveness in drug development, numerous studies have been conducted using computational methods (Neupane *et al*., 2024; Nairat *et al*., 2022; Abdessadak *et al*., 2022). It proposes to identify the putative binding mode and binding affinity between the ligands and the receptors (Haddou *et al*., 2023). Based on protein structures, numerous potential binding orientations within the active site are examined and assessed through molecular docking (Zhao *et al*., 2021). This work employs the extraction of phytocompounds from the fruits of *P. longum* followed by GC-MS analysis, molecular docking calculation, and ADMET prediction. The aim of this research work is to identify and propose potential inhibitors of α-amylase and α-glucosidase enzymes from plant-based resources.

2. Methodology

2.1 Chemicals

Hexane (Fischer Scientific), ethyl acetate (Fischer Scientific), and methanol (Fischer Scientific) of laboratory grade were used.

2.2 Preparation of plant extracts

The fruit of *P. longum* was collected from the Chitwan, Nepal and the collected fruits were crushed into powder by using an electric grinder. The ultrasonic extraction process was carried out and different fruit extracts i.e., hexane extract, ethyl acetate extract, and methanol extract were obtained using solvents hexane, ethyl acetate, and methanol respectively through solid-liquid fractionation.

2.3 Phytochemical identification

Phytochemical screening aids in identifying bioactive chemicals and the phytochemicals present in the fruits of *P. longum* were identified using chemical methods based on the methodology given by Banu and Cathrine, 2015 (Banu & Cathrine, 2015).

2.4 Gas Chromatography-Mass Spectrometry (GC-MS) Analysis

Gas chromatography-mass spectrometry (GCMS) analysis was conducted using a GCMS-QP 2010 instrument, operating under specific conditions. Helium was chosen as the carrier gas, flowing through an Rtx-5MS column of dimensions 30m×0.25mm×0.25µm. The temperature program involved ramping from 80 °C to 300 °C, with hold times at 2.0 and 5.0 min, respectively. The temperatures of the ion source and interface were consistently maintained at 200 °C and 250 °C, and the identification of compounds was obtained through MS comparison.

2.5 In silico approach

2.5.1 Selection and preparation of ligand database

A database of 33 ligand, obtained from the GC-MS analysis of different extracts of *Piper longum* were prepared. The 3D structures and atom coordinates were obtained in sdf format from the PubChem database (Kim *et al*., 2023). It was converted to pdb format using the Avogardo software, and an energy minimization was carried out after the addition of hydrogen atoms (Hanwell *et al*., 2012). Then using AutoDock Tools, Gasteiger charges were added and it was converted to pdbqt format required for molecular docking (Morris *et al*., 2008).

2.5.2 Target selection and preparation

The crystal protein 3D structures of α-glucosidase (PDB ID: 5ZCC) and α-amylase (PDB ID: 2QV4) with an X-ray diffraction resolution of 1.70 Å and 1.97 Å, respectively, were obtained from the RCSB database (Berman *et al*., 2000). Swiss Modeling server having a GMQE value of 0.99 with 99.64% sequence identity was used to perform homology modeling of α-glucosidase protein (Waterhouse *et al*., 2018). The proteins were cleaned by removing water molecules, ions, co-crystallized ligands, and co-factors using the PyMol software (Yuan *et al*., 2017). Then, AutoDock Tools was used to convert it to pdbqt format after the addition of polar hydrogens and Kollman charge.

2.5.3 Molecular Docking Calculations

The binding poses between the ligand and the receptor was determined with molecular docking calculations using AutoDock Vina software (Trott & Olson, 2009). The scoring function based on six different interaction terms were used to rank different poses of the ligands. The energy range of 4 units, the number of modes of 20, and the exhaustiveness of 64 were selected as control parameters. The grid center of (14.761, 50.038, 20,977) and the box size of 46×44×46 $Å^3$ with 0.375 Å spacing were chosen for α-amylase. Whereas, for α-glucosidase, box size of 30×30×30 $Å^3$ and grid center of (-0.655, 53.715, 72.724) were employed. The best protein-ligand complex with maximum binding affinity was determined and subjected to further analysis.

A good RMSD value of 0.5 Å for α-glucosidase and 1.3 Å for α-amylase validated the molecular docking protocol (Jain, 2003; Li *et al*., 2010; Ramírez & Caballero, 2018). The superimposition of the native ligand with docked ligands of α-amylase and α-glucosidase is shown in **Figure 1**.

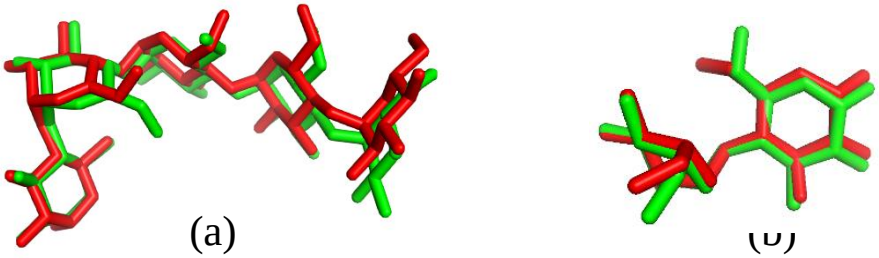

Figure 1. Superimposition of native ligand (green) with docked ligand (red) in (a) α-amylase and (b) α-glucosidase

2.5.4 ADMET predictions

Absorption, metabolism, excretion, distribution, and toxicity parameters were predicted using the ProTox-II, pkCSM, and ADMETlab 2.0 servers (Daina *et al*., 2014; Pires *et al*., 2015). Toxicity screening, including assessments for hepatotoxicity, cytotoxicity, mutagenicity, immunotoxicity, and LD50 value, was conducted using the ProTox-II server. The pkCSM server was utilized to ascertain drug pharmacokinetics, such as blood-brain barrier (BBB) permeability, central nervous system permeability (CNS), and gastrointestinal (GI) absorption. Additionally, the ADMETlab 2.0 server was employed for predicting Lipinski's rule (RO5) and total clearance value.

3. Results and Discussion

3.1 Phytochemical screening

The phytochemical analysis showed the presence of alkaloids, phenols, flavonoids, terpenoids, and volatile oils, as shown in **Table 1**. The terpenoids and volatile oils were present, whereas saponin was absent in all extracts. The methanol and ethyl acetate extracts showed a higher number of phytoconstituents than the hexane extract. Alkaloids, phenolic compounds, and flavonoids were found exclusively in the methanol and ethyl acetate extracts with their absence in the hexane extract, attributed to the varying polarity between the solvent employed and the plant's phytochemicals (Altemimi *et al*., 2017).

Table 1. Phytochemical analysis of the extracts

Class of Phytochemicals	Hexane extract	Ethyl acetate extract	Methanol extract
Volatile oil	+	+	+
Alkaloids	-	+	+
Phenols	-	+	+
Flavonoids	-	+	+
Terpenoids	+	+	+
Saponin	-	-	-

Here '+' refers presence and '-' refers absence

3.2 GC-MS analysis

The GC-MS chromatogram analysis exhibited 17 peaks in hexane extract, 24 peaks in ethyl acetate extract, and 6 peaks in methanol extract, as shown in the supplementary information (**Figure S1**). A total of 33 different compounds were obtained. The retention time, name, molecular formula, molecular weight, and area percentage of the obtained compounds were recorded as shown in **Table**

2-4. In hexane extract, decahydro-2-methylnaphthalene (17.06%) was the most prevalent compound, whereas in ethyl acetate extract, benzenepropanic acid (19.31%) was the primary compound.

Table 2. Compounds detected in hexane extract of fruits of *P. longum*

S.N.	Name of compounds	Molecular formula	Molecular weight	Retention time (min)	Area %
1	Caryophyllene	$C_{15}H_{24}$	204	13.495	3.97
2	α-Caryophyllene	$C_{15}H_{24}$	204	14.200	1.47
3	Germacrene D	$C_{15}H_{24}$	204	14.761	7.39
4	2,6,11-Trimethyldodecane	$C_{15}H_{32}$	212	14.961	3.55
5	1-methyl-4-(5-methy-1-methylene-4-hexenyl)- cyclohexane	$C_{15}H_{24}$	204	15.236	2.20
6	8-Heptadecene	$C_{17}H_{34}$	238	18.569	9.36
7	Heptadecane	$C_{17}H_{36}$	240	18.786	5.24
8	1-Nonadecane	$C_{19}H_{38}$	266	22.070	2.12
9	Bicyclo [2.2.1] heptane-1-methanesulfonic acid	$C_{10}H_{16}O_4S$	232	22.948	3.96
10	2-hydroxy-1-naphthalene carboxaldehyde	$C_{11}H_8O_2$	172	25.186	2.09
11	Decahydro-2-methylnaphthalene	$C_{11}H_{20}$	152	31.934	1.19
12	3,4-Methylenedioxyphenyl acetone	$C_{10}H_{10}O_3$	178	32.822	7.52
13	5,6-Dihydroergosterol	$C_{28}H_{46}O$	398	33.369	3.96
14	Piperine	$C_{17}H_{19}NO_3$	285	36.176	12.15
15	(E,E)-8,10-Dodecadien-1-ol	$C_{12}H_{22}O$	182	37.428	5.89

Table 3. List of compounds detected in ethyl acetate extract of fruits of *P. longum*

S.N.	Name of compounds	Molecular formula	Molecular weight	Retention time (min)	Area %
1	D-Mannitol	$C_6H_{14}O_6$	182	6.428	1.71
2	α-Isophoron	$C_9H_{14}O$	138	7.056	1.34
3	Acetoglyceride	$C_5H_{10}O_4$	134	9.655	0.90
4	Benzenepropanoic acid	$C_9H_{10}O_2$	150	11.959	19.31
5	(3Z)-3-Hexadecene	$C_{16}H_{32}$	224	12.739	2.27
6	2,4-di-tert-butyl-phenol	$C_{14}H_{22}O$	206	15.310	4.45
7	1-Heptadecanol	$C_{17}H_{36}O$	256	16.784	7.42
8	8-Heptadecene	$C_{17}H_{34}$	238	18.571	2.09
9	Hexadecane	$C_{16}H_{34}$	226	18.783	0.67
10	1-Nonadecene	$C_{19}H_{38}$	266	20.451	3.23
11	Pentadecanoic acid	$C_{15}H_{30}O_2$	242	23.341	5.70
12	2-hydroxy-1-naphthaldehyde	$C_{11}H_8O_2$	172	25.187	0.62
13	9-Tetradecenal	$C_{14}H_{26}O$	210	26.089	3.49
14	Diisooctyl phthalate	$C_{24}H_{38}O_4$	390	31.736	0.69
15	3,4-Methylenedioxyphenyl acetone	$C_{10}H_{10}O_3$	178	32.833	7.58
16	Piperine	$C_{17}H_{19}NO_3$	285	34.218	6.13
17	p-Menth-4(8)-en-3-one	$C_{10}H_{16}O$	152	36.946	0.90

The methanol extract of the fruit of *P. longum* contains 1, 3-Cyclohexadiene, 1-methyl-4-(1-methylethyl) as the most abundant phytocomponent with an area percentage of 66.12%. The mass spectra of each phytocompounds identified by GC-MS are presented in the supplementary information (**Figure S2-S4**). More than one peak for the same compound at different retention time might be due to various operational factors like the nature of carrier gas, temperature, and polarity of the stationary phase (Bizzo *et al*., 2023).

Table 4. List of compounds detected in methanol extract of fruits of *P. longum*

S. N.	Name of compounds	Molecular formula	Molecular weight	Retention time (min)	Area%
1	α-Terpinen	$C_{10}H_{16}$	136	9.609	66.12
2	p-Menthane	$C_{10}H_{16}O_2$	168	11.059	5.18
3	Phytol	$C_{20}H_{40}O$	296	13.068	4.11
4	β-Sitosterol	$C_{29}H_{50}O$	414	33.487	16.55
5	Squalene	$C_{30}H_{50}$	410	35.097	3.93
6	Tetrapentacontane	$C_{54}H_{110}$	758	35.417	4.11

3.3 Analysis of Computational Outputs

3.3.1 Molecular docking scores

A protein can bind a ligand at an orthosteric pocket based on the size, structure, functional groups, and interactions (Cele *et al*., 2022). Molecular docking determines the possibility and compatibility of interactions between a protein (host) and ligand (guest) in a complex (Faris *et al*., 2023). The effectiveness of the natural compounds as inhibitors relies on their binding affinities with the target protein. Although the correlation between binding affinity and inhibitory potential may not be straightforward in all cases, research has underscored the significance of comprehending the structural interactions between inhibitors and enzymes to formulate successful therapeutic strategies as discussed by Xu et al (Xu *et al*., 2016). Molecular docking of the studied compounds on α-amylase and α-glucosidase exhibited the best binding affinity with 5,6-dihydroergosterol, β-sitosterol, and piperine as shown in **Table 5**.

Table 5. Binding affinities of different compounds obtained from GCMS analysis of hexane, ethyl acetate, and methanol extracts along with native and reference drugs with α-amylase and α-glucosidase protein

Extracts	Ligands	Binding affinity (kcal/mol)	
		α-amylase	α-glucosidase
Hexane	5,6-Dihydroergosterol	-9.7	-9.1
	Piperine	-7.9	-8.1
	Caryophyllene	-7.0	-6.5
	Germacrene D	-7.0	-7.5
	α-Caryophyllene	-7.0	-6.2
	2-hydroxy-1-naphthalene carboxaldehyde	-6.7	-6.6

	Bicyclo[2.2.1]heptane-1-methanesulfonic acid	-6.5	-5.6
	Decahydro-2-methylnaphthalene	-6.2	-6.2
	3,4-Methylenedioxyphenyl acetone	-6.0	-6.3
	(E,E)-8,10-Dodecadien-1-ol	-5.7	-5.8
	2,6,11-Trimethyldodecane	-5.5	-5.7
	8-Heptadecene	-5.0	-5.4
	Heptadecane	-4.9	-5.2
	1-Nonadecene	-4.8	-5.2
Ethyl acetate	Piperine	-7.9	-8.1
	Diisooctyl phthalate	-6.9	-6.4
	2-hydroxy-1-naphthaldehyde	-6.7	-6.6
	2,4-di-tert-butyl-Phenol	-6.5	-6.6
	3,4-Methylenedioxyphenyl acetone	-6.1	-6.3
	Benzenepropanoic acid	-6.0	-6.6
	α-Isophoron	-5.4	-6.1
	D-Mannitol	-5.3	-5.7
	(3Z)-3-Hexadecene	-5.2	-5.2
	Pentadecanoic acid	-5.1	-5.7
	9-Tetradecenal	-5.1	-5.1
	8-Heptadecene	-5.0	-5.4
	Hexadecane	-4.8	-4.9
	1-Heptadecanol	-4.8	-5.1
	1-Nonadecene	-4.8	-5.2
	Acetoglyceride	-4.7	-4.8
Methanol	β-Sitosterol	-9.5	-9.4
	Squalene	-7.5	-7.0
	Phytol	-6.4	-6.6
	p-Menthane	-5.8	-6.1
	α-Terpinen	-5.7	-6.2
	Tetrapentacontane	-4.9	-4.6
	Miglitol	-5.8	-5.5

Reference Drugs	Voglibose	-6.1	-6.1
	Metformin	-5.4	-5.2
	Acarbose	-7.6	-7.8
	Native ligand	-10.4	-8.6

In the case of α-glucosidase, the binding affinity of -9.4 kcal/mol, -9.1 kcal/mol, and -8.1 kcal/mol were observed with β-sitosterol, 5,6-dihydroergosterol, and piperine, respectively. Whereas, molecular docking of ligands 5,6-dihydroergosterol, β-sitosterol and piperine with α-amylase protein demonstrated significant binding affinity of -9.7 kcal/mol, -9.5 kcal/mol, and -7.9 kcal/mol respectively. Some of the studied ligands showed better binding affinities with α-glucosidase than that of native having a binding affinity of -8.6 kcal/mol. However, none of the ligands showed a higher binding affinity with α-amylase than that of native having -10.4 kcal/mol. The majority of ligands exhibited higher binding affinities than that of the reference drugs (voglibose, miglitol, and metformin), indicating their better binding with both receptor proteins.

3.3.2 Protein-ligand interactions

3.3.2.1 α-amylase and ligand interactions

Numerous interactions such as alkyl, Pi-alkyl, Pi-Pi stacked, Pi-sigma, and van der Waals were observed between the ligands and α-amylase, as shown in **Figure 2** and **Table 6**. All the ligands showed hydrophobic interactions as there is no formation of any hydrogen bond representing the less polar nature of ligands. The hydrophobic interaction plays a significant role in ligand-α-amylase interaction (Liu *et al*., 2021). The major interaction was Pi-alkyl interaction shown by TRP59 in all three ligands, followed by alkyl interaction exhibited by LEU162 in 5,6-dihydroergosterol and β-sitosterol. In the case of piperine, the ligand reacted with amino acid residue ILE51 and TYR62 forming alkyl and Pi-pi stacked interaction. Pi-sigma interaction was formed between the ligand β-sitosterol and TRP59 amino acid residue. hydrophobic interaction with amino acid residues: TRP59 and TYR62 were also frequently observed in other literature and are analogous to our findings (Ogunyemi *et al*., 2022). Non-polar amino acid residues prefer non-polar ligands. In this regard, TRP with non-polar side group at the orthosteric pocket has facilitated the formation of multiple hydrophobic interactions with the alkyl groups (non-polar) of the docked ligands (**Figure 2**). The catalytic triad, ASP197, GLU233, and ASP300 showed van der Waals interaction with 5,6-dihydroergosterol whereas (GLU233, ASP300) and (ASP197, ASP300) exhibited van der Waals interaction with β-sitosterol and piperine demonstrating that the ligands have interacted with α-amylase at the same pocket.

3.3.2.2 α-glucosidase and ligand interactions

In the case of α-glucosidase protein adducts, numerous interactions such as hydrogen bond, carbon-hydrogen bond, alkyl, Pi-alkyl, Pi-sigma, Pi-sulfur, and van der Waals were observed as shown in **Figure 3** and **Table 7**. β-sitosterol, and piperine showed both hydrophilic and hydrophobic interaction due to the presence of hydrogen bonds (Nakagawa & Tamada, 2021) whereas 5,6-dihydroergosterol exhibited only hydrophobic interaction. In β-sitosterol-protein complex, the ligand interacted with amino acid residues ASP382 and GLY410 forming a conventional hydrogen bond

and carbon-hydrogen bond, respectively. Similarly, Pi-sigma and alkyl interaction were observed with (TYR63, PHE162), and (ILE143, MET385, and ARG411) respectively. Pi-alkyl interactions of β-Sitosterol and 5,6-dihydroergosterol were seen with HIS203, and PHE282 whereas ILE143 and MET385 displayed alkyl interactions.

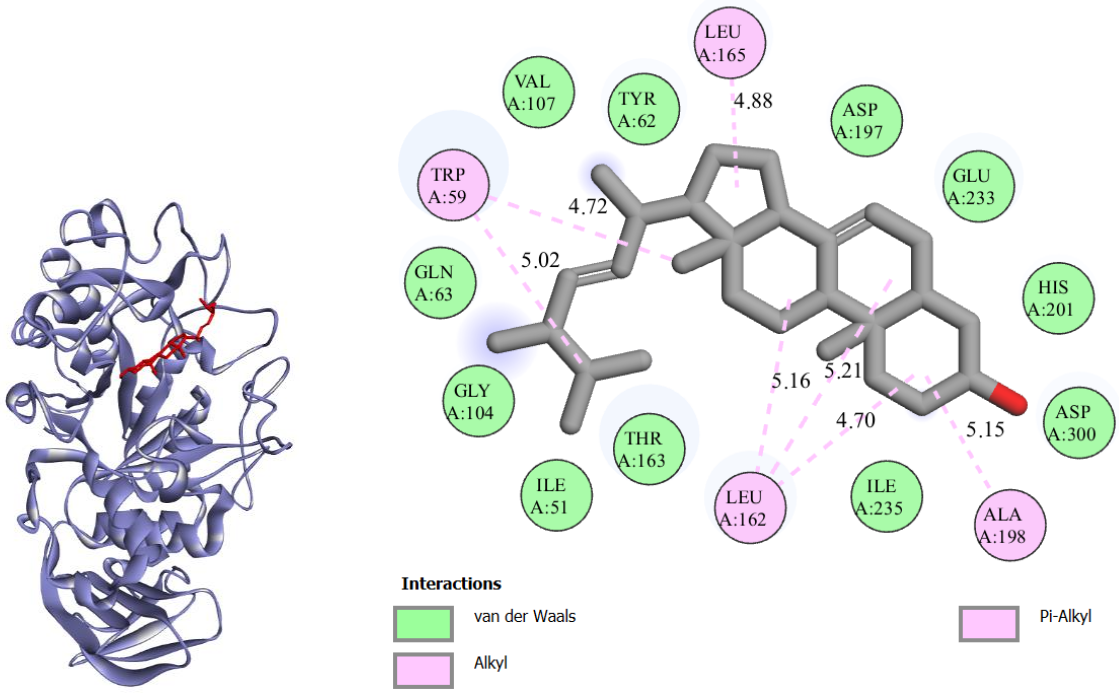

(A)

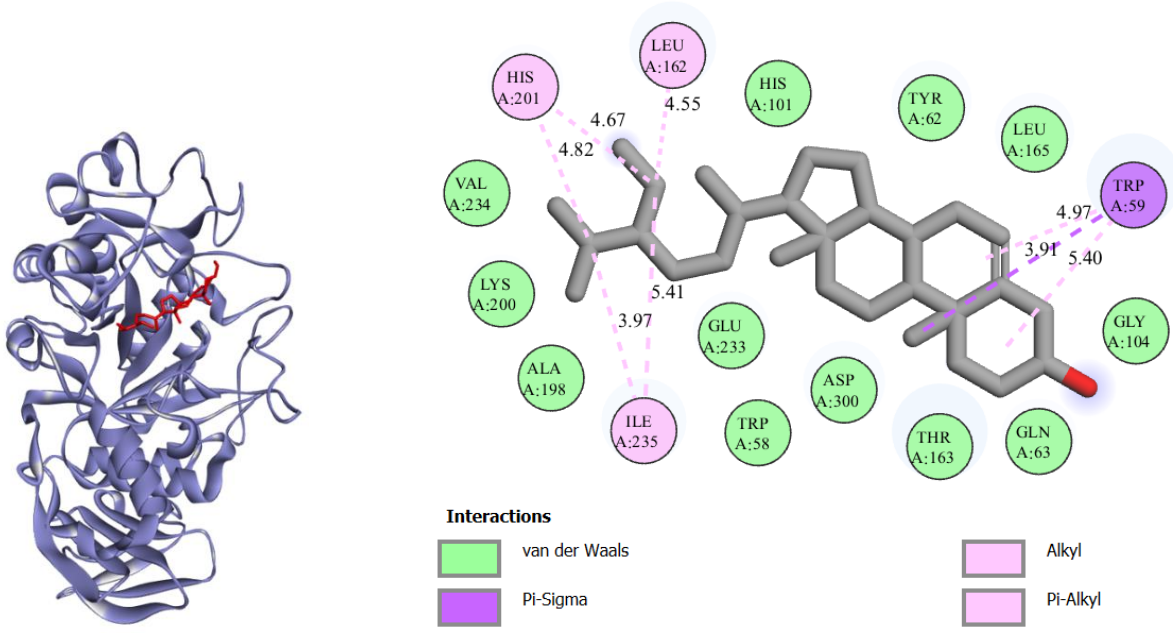

(B)

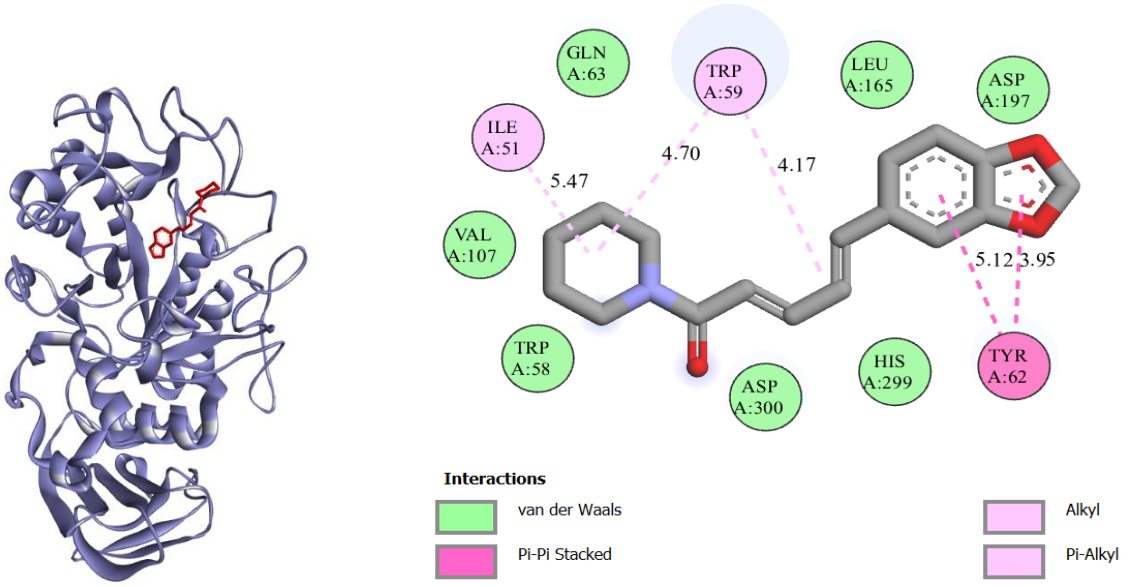

(C)

Figure 2. 2D interaction (right) and 3D docked ligand at the binding site (left) of **(A)** 5,6-Dihydroergosterol, **(B)** β-Sitosterol, and **(C)** Piperine with α-amylase

In the piperine-protein complex, amino acid residue GLN256 interacted by forming hydrogen bonds whereas Pi-alkyl and alkyl interactions were seen with TYR63, PHE163, and ALA200 respectively. Similarly, MET385 interacted with two aromatic rings of the piperine to form Pi-sulfur bonds. Moreover, several van der Waals interactions were observed between all three top ligands and amino acid residues. The major interactions of the ligands with the amino acids of both receptors showed hydrophobic binding at the orthosteric pocket, concluding the nonpolar nature of the compounds obtained from the GCMS analysis.

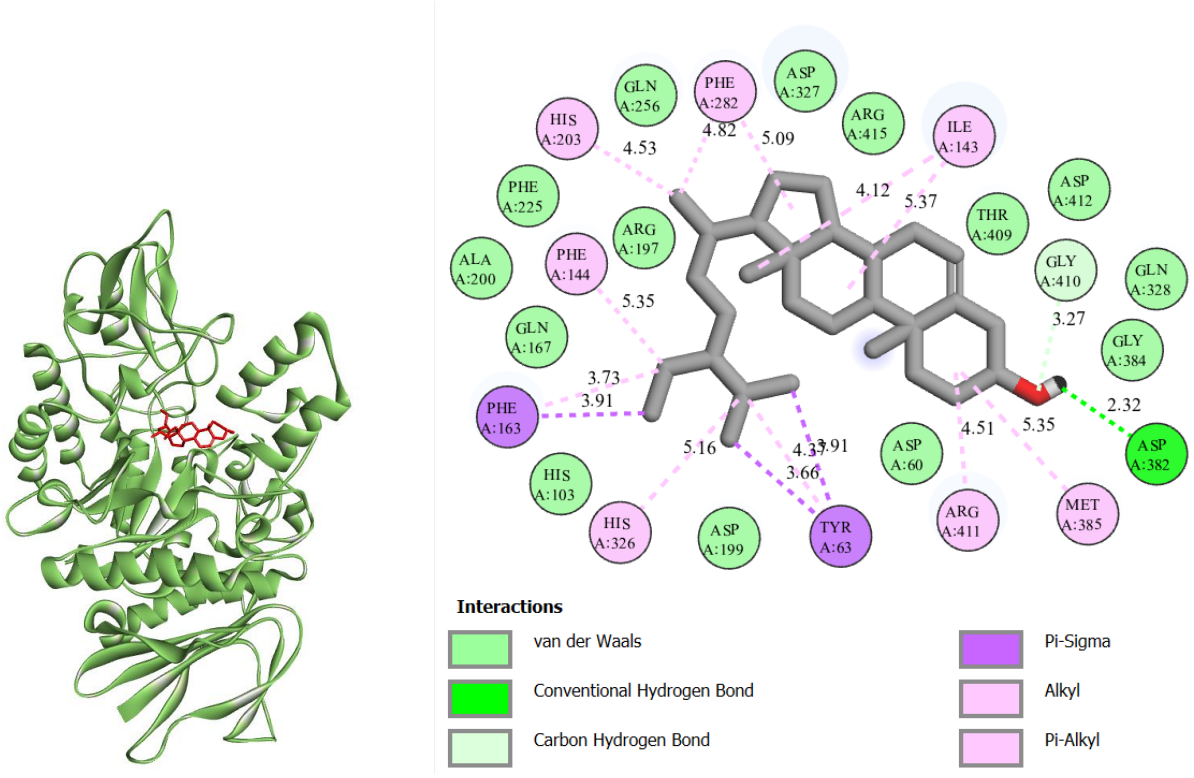

(A)

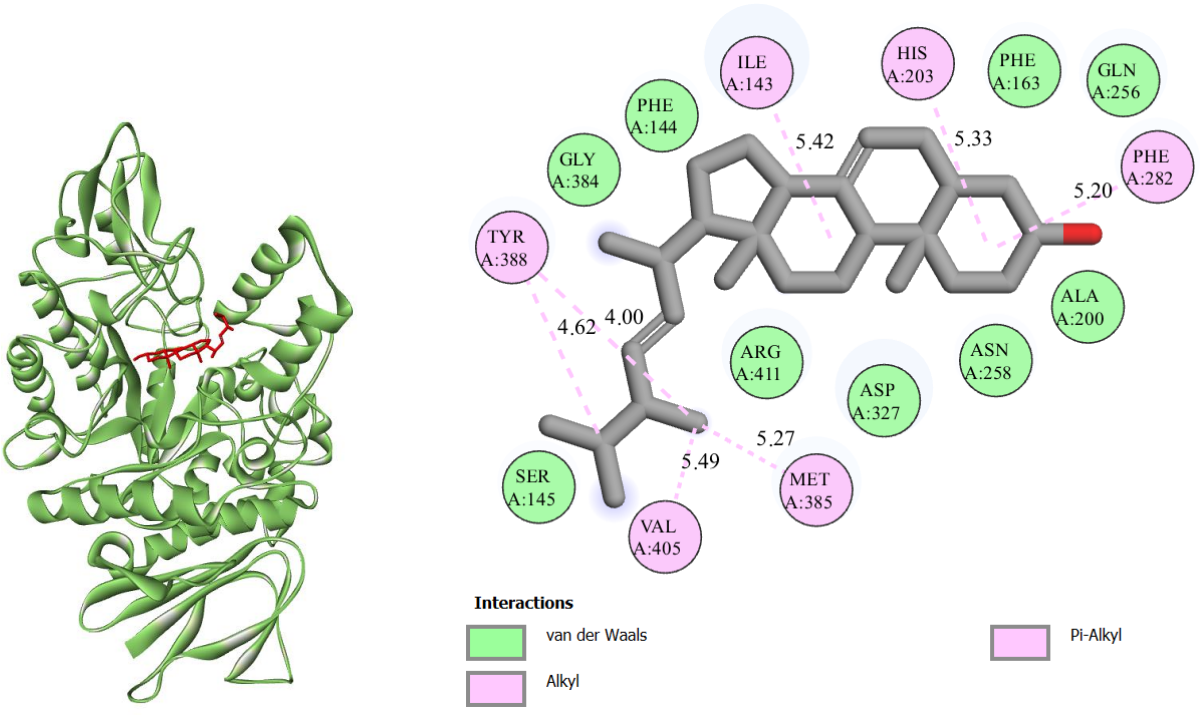

(B)

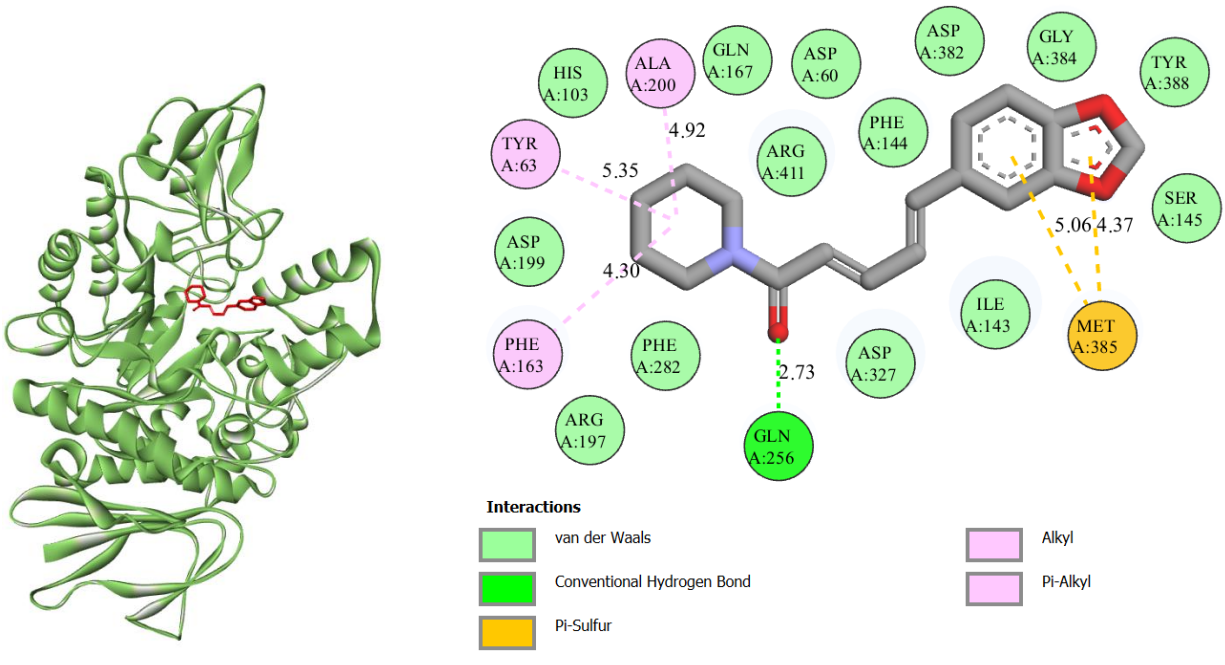

(C)

Figure 3. 2D projection of interactions (right) and 3D docked ligand at the binding site (left) of **(A)** β-Sitosterol, **(B)** 5,6-Dihydroergosterol, and **(C)** Piperine with α-glucosidase

Table 6. Top three protein-ligand complexes and their respective interactions with amino acid residues of α-amylase

Ligands	Types of interactions	Active site residues (Distance Å)
5,6-Dihydroergosterol	Pi-alkyl	TRP59 (4.72, 5.02)
	Alkyl	LEU162 (4.70, 5.16, 5.21), LEU165 (4.88), ALA198 (5.15)
	van der Waals	ILE51, TYR62, GLN63, GLY104, VAL107, THR163, ASP197, HIS201, GLU233, ILE235, ASP300
β-Sitosterol	Pi-Alkyl	TRP59 (4.97, 5.40), HIS201 (4.67, 4.82)
	Alkyl	LEU162 (4.55), ILE235 (3.97,5.41)
	Pi-Sigma	TRP59 (3.91)
	van der Waals	TRP58, TYR62, GLN63, HIS101, GLY104, THR163, LEU165, ALA198, LYS200, GLU233, VAL234, ASP300
Piperine	Pi-Alkyl	TRP59 (4.17, 4.70)
	Alkyl	ILE51 (5.47)
	Pi-Pi Stacked	TYR62 (3.95, 5.12)
	van der Waals	TRP58, GLN63, VAL107, LEU165, ASP197, HIS299, ASP300

Table 7. Top three protein-ligand complexes and their respective interactions with amino acid residues of α-glucosidase

Ligands	Types of interactions	Active site residues (Distance Å)
β-Sitosterol	Hydrogen Bond	ASP382 (2.32)
	Carbon-hydrogen Bond	GLY410 (3.27)
	Pi-Alkyl	TYR63 (4.37), PHE144 (5.35), PHE163 (3.73), HIS203 (4.53), PHE282 (4.82, 5.09), HIS326 (5.16)
	Alkyl	ILE143 (4.12, 5.37), MET385 (5.35), ARG411 (4.51)
	Pi-Sigma	TYR63 (3.66, 3.91), PHE163 (3.91)
	van der Waals	ASP60, HIS103, GLN167, ARG197, ASP199, ALA200, PHE225, GLN256, ASP327, GLN328, GLY384, THR409, ASP412, ARG415
5,6-Dihydroergosterol	Pi-alkyl	HIS203 (5.33), PHE282 (5.20), TYR388 (4.00, 4.62)
	Alkyl	ILE143 (5.42), MET385 (5.27), VAL405 (5.49)

	van der Waals	PHE144, SER145, PHE163, ALA200, GLN256, ASN258, ASP327, GLY384, ARG411
Piperine	Hydrogen Bond	GLN256 (2.73)
	Pi-Alkyl	TYR63 (5.35), PHE163 (4.30)
	Alkyl	ALA200 (4.92)
	Pi-Sulfur	MET385 (4.37, 5.06)
	van der Waals	ASP60, HIS103, ILE143, PHE144, SER145, GLN167, ARG197, ASP199, PHE282, ASP327, ASP382, GLY384, TYR388, ARG411

3.3.3 Drug likeness and safety profile

The ADMET profile of the top three ligands and four reference drugs is shown in **Table 8**. All three compounds investigated in this study lied under toxicity class 4, displaying their toxic nature (Banerjee *et al*., 2018), which aligns with that of the reference drugs milglitol and metformin. The predicted lethal dose of 50% (LD50) was found to be 890 mg/kg and more for 5,6-dihydroergosterol and β-sitosterol except for piperine having 330 mg/kg. The compounds adhered to Lipinski's Rule of Five, indicating a likelihood of drug-like properties (Benet *et al*., 2016). In contrast, the reference drug acarbose did not comply with the rule.

Table 8. ADMET analysis of the top three ligands and four reference drugs

ADMET parameters	**Compounds**						
	5,6-Dihydro ergosterol	**β-Sitosterol**	**Piperine**	**Miglitol**	**Metformin**	**Voglibose**	**Acarbose**
Toxicity class	4	4	4	4	4	6	6
LD_{50} (mg/kg)	2000	890	330	1200	680	14700	24000
Lipinski rule (RO5)	Yes	Yes	Yes	Yes	Yes	Yes	No
Immunotoxicity	Active	Active	Active	Inactive	Inactive	Inactive	Active
Hepatotoxicity	Inactive	Inactive	Inactive	Inactive	Inactive	Inactive	Mildly active
Carcinogenicity	Inactive	Inactive	Mildly active	Inactive	Inactive	Inactive	Inactive
Mutagenicity	Inactive	Inactive	Inactive	Inactive	Inactive	Inactive	Inactive
Cytotoxicity	Inactive	Inactive	Inactive	Inactive	Inactive	Inactive	Inactive
BBB penetration	Yes	Yes	Yes	No	Yes	No	No
CNS permeability	Yes	Yes	Yes	No	No	No	No
Intestinal absorption	High	High	High	Moderate	Moderate	Low	Low
Total Clearance (ml/min/kg)	17.724	16.686	10.873	2.006	3.531	1.577	0.373

The studied compounds exhibited immunotoxicity, suggesting the possibility of causing harm or interference with the regular operation of the immune system, similar to acarbose (Zerdan *et al*., 2021). They were found to be non-mutagenic, non-cytotoxic, and non-hepatotoxic. Similarly, the majority of phytochemicals showed non-carcinogenicity except piperine. Pharmacokinetics (ADME) data revealed that the compounds could penetrate the blood-brain barrier and central nervous system (Carpenter *et al*., 2014). The three compounds demonstrated optimal or high gastrointestinal absorption, suggesting that their chemical structures, molecular weights, solubilities, and sizes are adequate for absorption into the bloodstream from the gastrointestinal tract (Azman *et al*., 2022). High to moderate total renal clearance was observed for the studied compounds. In contrast, moderate to low gastrointestinal absorption and low renal clearance were demonstrated by the reference drugs. Hence, through a comparative assessment of toxicities and pharmacokinetics with reference drugs, the compounds could be proposed as potential candidates for diabetes medication. The findings highlighted that the phytochemicals exhibited drug-like characteristics, aligning with or surpassing at least one of the drug molecules in nearly all ADMET parameters. The results propose the need for further in vitro and in vivo experiments to validate the drug-like attributes and safety of the compounds.

Therapeutic effects such as reduction in hyperglycemia through the potential inhibition of α-amylase and α-glucosidase enzymes through stronger binding with the catalytic pocket (higher binding affinity relative to the reference molecule) and halting the normal functioning of the proteins. From the ADMET prediction, concerns such as Blood blood-brain barrier (BBB) penetration, Central Nervous System (CNS) permeability, and immunotoxicity were raised. However, additional experimental trials on animal model is required in order to address these ADMET concerns.

The study explored the phytochemical composition of *Piper longum* fruit extracts, identifying various compounds like alkaloids, phenols, flavonoids, terpenoids, and volatile oils through phytochemical screening and GC-MS analysis. Hexane and ethyl acetate extracts showed a higher number of phytoconstituents than the methanol extract, with distinct compounds such as decahydro-2-methylnaphthalene and β-sitosterol. Molecular docking studies suggested potential therapeutic effects against diabetes, but ADMET analysis raised concerns about toxicity, emphasizing the need for further experimental trials to validate the safety and efficacy of these phytochemicals for diabetes management.

Conclusion

From a pool of 33 different compounds obtained from GC-MS analysis of *Piper longum*, 5,6-dihydroergosterol, β-sitosterol, and piperine showed stronger binding at the orthosteric pocket of α-amylase and α-glucosidase enzymes compared to that of the reference drugs and native ligands. These phytocompounds exhibited considerable toxicity and drug-likeness comparable to that of the reference drugs. The hit compounds, especially 5,6-dihydroergosterol could be proposed for further experimental trials and pharmacophore modeling in the course of developing drug-like molecules for the management of diabetes mellitus. Therefore, plant-based resources with ethnobotanical and traditional values could be implemented in the modern scientific drug design and development.

Acknowledgement: The authors would like to acknowledge the Department of Food Technology and Quality Control, Kathmandu, Nepal for GC-MS experiments.

Disclosure statement: *Conflict of Interest:* The authors declare that there are no conflicts of interest. *Compliance with Ethical Standards:* This article does not contain any studies involving human or animal subjects.

References

Abdessadak O., Hajji H., Mehanned S., Ajana M. A., Lakhlifi T., & Bouachrine M. (2022). Reverse docking on five original PPO structures: Plant, Bacterial, and human. *Moroccan Journal of Chemistry*, 10(3), 10-3. https://doi.org/10.48317/IMIST.PRSM/morjchem-v10i3.33065

Altemimi A., Lakhssassi N., Baharlouei A., Watson D. G., & Lightfoot D. A. (2017). Phytochemicals: Extraction, isolation, and identification of bioactive compounds from plant extracts. *Plants*, 6(4). https://doi.org/10.3390/plants6040042

Azman M., Sabri A. H., Anjani Q. K., Mustaffa M. F., & Hamid K. A. (2022). Intestinal Absorption Study: Challenges and Absorption Enhancement Strategies in Improving Oral Drug Delivery. *Pharmaceuticals*, 15(8). https://doi.org/10.3390/ph15080975

Gaikwad S., Krishna Mohan G., & Rani M. S. (2014). Phytochemicals for Diabetes Management. *Pharmaceutical Crops*, 5(1), 11–28. https://doi.org/10.2174/2210290601405010011

Babu K. N., Divakaran M., Ravindran P. N., & Peter K. V. (1976). Long pepper. *Handbook of herbs and spices*. Woodhead Publishing Limited. https://doi.org/10.1533/9781845691717.3.420

Banerjee P., Eckert A. O., Schrey A. K., & Preissner R. (2018). ProTox-II: A webserver for the prediction of toxicity of chemicals. *Nucleic Acids Research*, 46(W1), W257–W263. https://doi.org/10.1093/nar/gky318

Banu K. S., & Cathrine L. (2015). General Techniques Involved in Phytochemical Analysis. *International Journal of Advanced Research in Chemical Science*, 2(4), 25–32.

Benet L. Z., Hosey C. M., Ursu O., & Oprea T. I. (2016). BDDCS, the Rule of 5 and drugability. *Advanced Drug Delivery Reviews*. 101, 89-98. https://doi.org/10.1016/j.addr.2016.05.007

Berman H. M., Westbrook J., Feng Z., Gilliland G., Bhat T. N., Weissig H., Shindyalov I. N., & Bourne P. E. (2000). The Protein Data Bank. *Nucleic Acids Research*, 28(1), 235-242.

Bizzo H. R., Brilhante N. S., Nolvachai Y., & Marriott P. J. (2023). Use and abuse of retention indices in gas chromatography. *Journal of Chromatography A*, 464376. https://doi.org/10.1016/j.chroma.2023.464376

Carpenter T. S., Kirshner D. A., Lau E. Y., Wong S. E., Nilmeier J. P., & Lightstone F. C. (2014). A Method to Predict Blood-Brain Barrier Permeability of Drug-Like Compounds Using Molecular Dynamics Simulations. *Biophysical Journal*, 107(3), 630–641. https://doi.org/10.1016/j.bpj.2014.06.024

Carsono N., Tumilaar S. G., Kurnia D., Latipudin D., & Satari M. H. (2022). A Review of Bioactive Compounds and Antioxidant Activity Properties of Piper Species. *Molecules*, 27(19), 1–22. https://doi.org/10.3390/molecules27196774

Cele N., Awolade P., Seboletswe P., Olofinsan K., Islam M. S., & Singh P. (2022). α-Glucosidase and α-Amylase Inhibitory Potentials of Quinoline–1,3,4-oxadiazole Conjugates Bearing 1,2,3-Triazole with Antioxidant Activity, Kinetic Studies, and Computational Validation. *Pharmaceuticals*, 15(8). https://doi.org/10.3390/ph15081035

Chintoju N., Konduru P., Kathula R. L., & Remella R. (2015). Importance of Natural Products in the Modern History. *Research & Reviews: Journal of Hospital and Clinical Pharmacy*, 1(1), 5–10.

Coman C., Rugină O. D., & Socaciu C. (2012). Plants and natural compounds with antidiabetic action. *Notulae Botanicae Horti Agrobotanici Cluj-Napoca*, 40(1), 314–325. https://doi.org/10.15835/nbha4017205

Daina A., Michielin O., & Zoete V. (2014). ILOGP: A simple, robust, and efficient description of n-octanol/water partition coefficient for drug design using the GB/SA approach. *Journal of Chemical Information and Modeling*, 54(12), 3284–3301. https://doi.org/10.1021/ci500467k

Duraipandiyan V., Ayyanar M., & Ignacimuthu S. (2006). Antimicrobial activity of some ethnomedicinal plants used by Paliyar tribe from Tamil Nadu, India. *BMC Complementary and Alternative Medicine*, 6, 1-7. https://doi.org/10.1186/1472-6882-6-35

Faris A., Edder Y., Louchachha I., Lahcen I. A., Azzaoui K., Hammouti B., Merzouki M., Challioui A., Boualy B., Karim A., Hanbali G., & Jodeh S. (2023). From himachalenes to trans-himachalol: unveiling bioactivity through hemisynthesis and molecular docking analysis. *Scientific reports*, 13(1), 17653. https://doi.org/10.1038/s41598-023-44652-z

Grenda A., Jakubczyk A., Kiersnowska K., & Rybczy K. (2023). Natural Compounds with Antimicrobial Properties in Cosmetics. *Pathogens*, 12(2), 320.

Haddou S., Mounime K., Loukili E., *et al*. (2023). Investigating the Biological Activities of Moroccan Cannabis Sativa L Seed Extracts: Antimicrobial, Anti-inflammatory, and Antioxidant Effects with Molecular Docking Analysis. *Moroccan Journal of Chemistry*, 11(04), 11-4. https://doi.org/10.48317/IMIST.PRSM/morjchem-v11i04.42100

Haddou S., Elrherabi A., Loukili E.H. *et al.* (2024) Chemical Analysis of the Antihyperglycemic, and Pancreatic α-Amylase, Lipase, and Intestinal α-Glucosidase Inhibitory Activities of Cannabis sativa L. Seed Extracts. *Molecules*, 29, 93. https://doi.org/10.3390/molecules29010093

Hanwell M. D., Curtis D. E., Lonie D. C., Vandermeerschd T., Zurek E., & Hutchison G. R. (2012). Avogadro: An advanced semantic chemical editor, visualization, and analysis platform. *Journal of Cheminformatics*, 4(1), 1-17. https://doi.org/10.1186/1758-2946-4-17

Jain A. N. (2003). Surflex: Fully automatic flexible molecular docking using a molecular similarity-based search engine. *Journal of Medicinal Chemistry*, 46(4), 499–511. https://doi.org/10.1021/jm020406h

Kajaria D., Tripathi J., Tripathi Y.B., & Tiwari S. (2013). In-vitro α amylase and glycosidase inhibitory effect of ethanolic extract of antiasthmatic drug — Shirishadi. *Journal of Advanced Pharmaceuticals Technology and Research*, 4(4), 206. https://doi.org/10.4103/2231-4040.121415

Kaushik D., Rani R., Kaushik P., Sacher D., & Yadav J. (2012). In vivo and in vitro antiasthmatic studies of plant *Piper longum* Linn. *International Journal of Pharmacology*, 8(3), 192–197. https://doi.org/10.3923/ijp.2012.192.197

Khaldan A., Bouamrane S., El Mchichi R. E. M. L., Maghat H., Lakhlifi M. B. T., & Sbai A. (2022). In search of new potent α-glucosidase inhibitors: molecular docking and ADMET prediction. *Moroccan Journal of Chemistry*, 10(4), 10-4. https://doi.org/10.48317/IMIST.PRSM/morjchem-v10i4.34702

Khushbu C., Roshni S., Anar P., Carol M., & Mayuree P. (2011). Phytochimical and therapeutic potential of *piper longum* linn. *International Journal of Research in Ayurveda & Pharmacy*, 2(1), 161.

Kim S., Chen J., Cheng T., Gindulyte A., He J., He S., Li Q., Shoemaker B. A., Thiessen P. A., Yu B., Zaslavsky L., Zhang J., & Bolton E. E. (2023). PubChem 2023 update. *Nucleic Acids Research*, 51(D1), D1373–D1380.

Kumar S., Kamboj J., & Sharma S. (2011). Overview for Various Aspects of the Health Benefits of *Piper Longum* Linn. Fruit. *Journal of Acupuncture and Meridian Studies*, 4(2), 134–140. https://doi.org/10.1016/S2005-2901(11)60020-4

Kumar S., Sharma S., & Vasudeva N. (2013). Screening of antidiabetic and antihyperlipidemic potential of oil from *Piper longum* and piperine with their possible mechanism. *Expert Opinion on Pharmacotherapy*, 14(13), 1723–1736. https://doi.org/10.1517/14656566.2013.815725

Li D., Wang R., Cheng X., Yang J., Yang Y., Qu H., Li S., Lin S., Wei D., Bai Y., & Zheng X. (2022). Chemical constituents from the fruits of *Piper longum* L. and their vascular relaxation

effect on rat mesenteric arteries. *Natural Product Research*, 36(2), 674–679. https://doi.org/10.1080/14786419.2020.1797726

Li X., Li Y., Cheng T., Liu Z., & Wang R. (2010). Evaluation of the performance of four molecular docking programs on a diverse set of protein-ligand complexes. *Journal of Computational Chemistry*, 31(11), 2109–2125. https://doi.org/10.1002/jcc.21498

Liu Q. Z., Zhang H., Dai H. Q., Zhao P., Mao Y. F., Chen K. X., & Chen Z. X. (2021). Inhibition of starch digestion: the role of hydrophobic domain of both α-amylase and substrates. *Food Chemistry*, 341, 128211. https://doi.org/10.1016/j.foodchem.2020.128211

Magaña-Barajas E., Buitimea-Cantúa G. V., *et al.* (2021). In vitro α-amylase and α-glucosidase enzyme inhibition and antioxidant activity by capsaicin and piperine from Capsicum Chinense and Piper nigrum fruits. *Journal of Environmental Science and Health - Part B Pesticides, Food Contaminants, and Agricultural Wastes*, 56(3), 282–291. https://doi.org/10.1080/03601234.2020.1869477

Morris G. M., Huey R., & Olson A. J. (2008). Using autodock for ligand-receptor docking. *Current protocols in bioinformatics*, 24(1), 8-14. https://doi.org/10.1002/0471250953.bi0814s24

Nabi S. A., Kasetti R. B., Sirasanagandla S., Tilak T. K., Kumar M. V. J., & Rao C. A. (2013). Antidiabetic and antihyperlipidemic activity of *Piper longum* root aqueous extract in STZ induced diabetic rats. *BMC Complementary and Alternative Medicine*, 13, 1-9. https://doi.org/10.1186/1472-6882-13-37

Nairat N., Hamed O., Berisha A., Jodeh S., Algarra M., Azzaoui K., Dagdag O., et al. (2022) Cellulose polymers with β-amino ester pendant group: design, synthesis, molecular docking and application in adsorption of toxic metals from wastewater, *BMC Chemistry* 16 (1), 1-21

Nakagawa H., & Tamada T. (2021). Hydration and its Hydrogen Bonding State on a Protein Surface in the Crystalline State as Revealed by Molecular Dynamics Simulation. *Frontiers in Chemistry*, 9, 1–7. https://doi.org/10.3389/fchem.2021.738077

Neupane P., Adhikari Subin J., & Adhikari R. (2024). Assessment of iridoids and their similar structures as antineoplastic drugs by in silico approach. *Journal of Biomolecular Structure and Dynamics*, 1–16. https://doi.org/10.1080/07391102.2024.2314262

Neupane P., Dhital S., Parajuli N., Shrestha T., Bharati S., Maharjan B., Adhikari Subin J., & Shrestha R. L. S. (2023). Exploration of Anti-Diabetic Potential of Rubus ellipticus smith through Molecular Docking, Molecular Dynamics Simulation, and MMPBSA Calculation. *Journal of Nepal Physical Society*, 9(2), 95–105. doi.org/10.3126/jnphyssoc.v9i2.62410

Ogunyemi O. M., Gyebi G. A., Saheed A., Paul J., Nwaneri-Chidozie V., Olorundare O., Adebayo J., Koketsu M., Aljarba N., Alkahtani S., Batiha G. E., & Olaiya C. O. (2022). Inhibition mechanism of alpha-amylase, a diabetes target, by a steroidal pregnane and pregnane glycosides derived from Gongronema latifolium Benth. *Frontiers in Molecular Biosciences*, 9, 866719. https://doi.org/10.3389/fmolb.2022.866719

Pires D. E. V., Blundell T. L., & Ascher D. B. (2015). pkCSM: Predicting small-molecule pharmacokinetic and toxicity properties using graph-based signatures. *Journal of Medicinal Chemistry*, 58(9), 4066–4072. https://doi.org/10.1021/acs.jmedchem.5b00104

Priyadarshi A., Singh S., Singh B., & Sharma P. (2018). Pharmacognostical and phytochemical analysis of Pippali (*Piper longum* Linn.). *The Pharma Innovation Journal*, 7(6), 286–289.

Ramírez D., & Caballero J. (2018). Is It Reliable to Take the Molecular Docking Top Scoring Position as the Best Solution without Considering Available Structural Data? *Molecules*, 23(5), 1038. https://doi.org/10.3390/molecules23051038

Scott I. M., Jensen H. R., Philogène B. J. R., & Arnason J. T. (2008). A review of Piper spp. (Piperaceae) phytochemistry, insecticidal activity and mode of action. *Phytochemistry Reviews*, 7(1), 65–75. https://doi.org/10.1007/s11101-006-9058-5

Teoh S. L., & Das S. (2018). Phytochemicals and their effective role in the treatment of diabetes mellitus: a short review. *Phytochemistry Reviews*, 17(5), 1111–1128. https://doi.org/10.1007/s11101-018-9575-z

Tolmie M., Bester M. J., & Apostolides Z. (2021). Inhibition of α-glucosidase and α-amylase by herbal compounds for the treatment of type 2 diabetes: A validation of in silico reverse docking with in vitro enzyme assays. *Journal of Diabetes*, 13(10), 779–791. https://doi.org/10.1111/1753-0407.13163

Trott O., & Olson A. J. (2009). AutoDock Vina: Improving the speed and accuracy of docking with a new scoring function, efficient optimization, and multithreading. *Journal of Computational Chemistry*, 31(2), 455-461. https://doi.org/10.1002/jcc.21334

Waterhouse A., Bertoni M., Bienert S., Studer G., Tauriello G., Gumienny R., Heer F. T., De Beer T. A. P., Rempfer C., Bordoli L., Lepore R., & Schwede T. (2018). SWISS-MODEL: Homology modelling of protein structures and complexes. *Nucleic Acids Research*, 46(W1), W296–W303. https://doi.org/10.1093/nar/gky427

Xu W., Shao R., & Xiao J. (2016). Is there consistency between the binding affinity and inhibitory potential of natural polyphenols as α-amylase inhibitors?. *Critical reviews in food science and nutrition*, 56(10), 1630-1639. https://doi.org/10.1080/10408398.2013.793652

Yuan S., Chan H. C. S., & Hu Z. (2017). Using PyMOL as a platform for computational drug design. *Wiley Interdisciplinary Reviews: Computational Molecular Science*, 7(2). https://doi.org/10.1002/wcms.1298

Zerdan M. B., Moussa S., Atoui A., & Assi H. I. (2021). Mechanisms of immunotoxicity: Stressors and evaluators. *International Journal of Molecular Sciences*, 22(15), 8242. https://doi.org/10.3390/ijms22158242

Zhao Y., Wang M., & Huang G. (2021). Structure-activity relationship and interaction mechanism of nine structurally similar flavonoids and α-amylase. *Journal of Functional Foods*, 86, 104739. https://doi.org/10.1016/j.jff.2021.104739

Supplementary Information

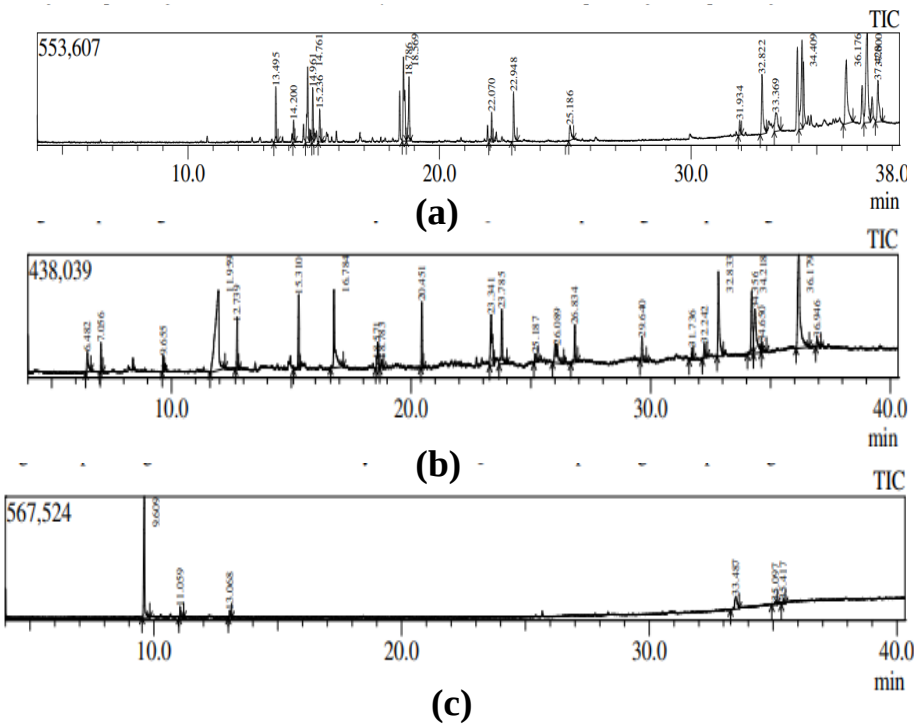

Figure S1. Chromatogram of (a) hexane, (b) ethyl acetate, and (c) methanol extracts

Mass Spectral Data of Constituents Identified by GC-MS in Hexane extract

SI:94 Formula:C15H24 CAS:87-44-5 MolWeight:204 RetIndex:1494
CompName:Caryophyllene $$ Bicyclo[7.2.0]undec-4-ene, 4,11,11-trimethyl-8-methylene-, [1R-(1R*

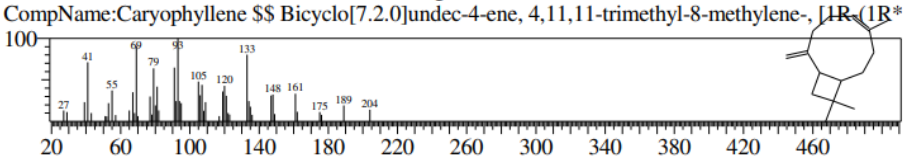

SI:93 Formula:C15H24 CAS:6753-98-6 MolWeight:204 RetIndex:1579
CompName:.alpha.-Caryophyllene $$ 1,4,8-Cycloundecatriene, 2,6,6,9-tetramethyl-, (E,E,E)- $$,alp

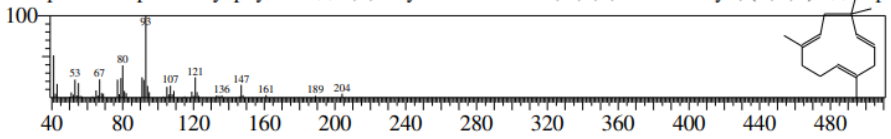

SI:90 Formula:C15H24 CAS:23986-74-5 MolWeight:204 RetIndex:1515
CompName:1,6-Cyclodecadiene, 1-methyl-5-methylene-8-(1-methylethyl)-, [s-(E,E)]- $$ Germacren

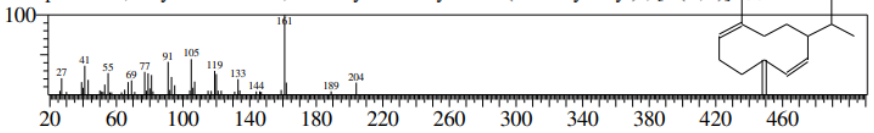

SI:84 Formula:C15H32 CAS:31295-56-4 MolWeight:212 RetIndex:1320
CompName:Dodecane, 2,6,11-trimethyl- $$ 2,6,11-Trimethyldodecane $$

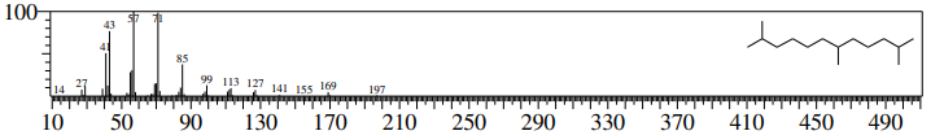

SI:94 Formula:C15H24 CAS:495-61-4 MolWeight:204 RetIndex:1500
CompName:Cyclohexene, 1-methyl-4-(5-methyl-1-methylene-4-hexenyl)-, (S)- $$ 1,5-Heptadiene, 6-

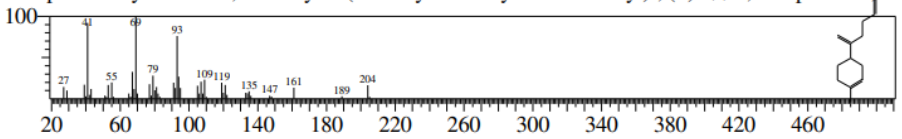

SI:92 Formula:C17H34 CAS:54290-12-9 MolWeight:238 RetIndex:1719
CompName:8-Heptadecene $$ (8E)-8-Heptadecene # $$

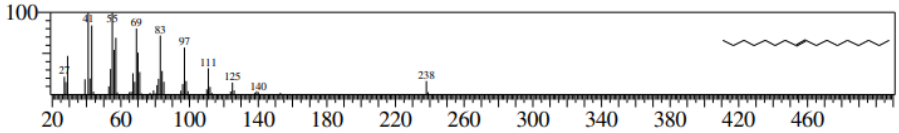

SI:93 Formula:C17H36 CAS:629-78-7 MolWeight:240 RetIndex:1711
CompName:Heptadecane $$ n-Heptadecane $$ Normal-heptadecane $$

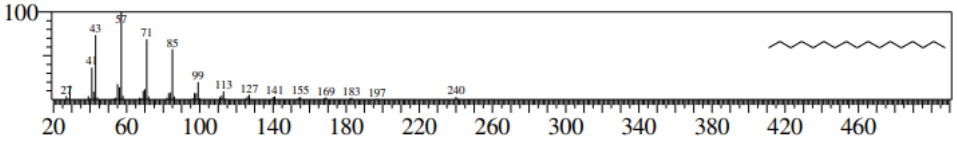

SI:93 Formula:C19H38 CAS:18435-45-5 MolWeight:266 RetIndex:1900
CompName:1-Nonadecene

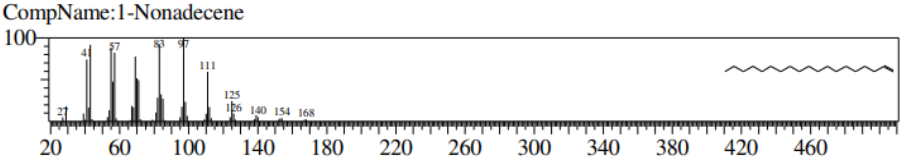

SI:72 Formula:C10H16O4S CAS:5872-08-2 MolWeight:232 RetIndex:1767
CompName:Bicyclo[2.2.1]heptane-1-methanesulfonic acid, 7,7-dimethyl-2-oxo-, (.+/-.)- $$ Bicyclo[

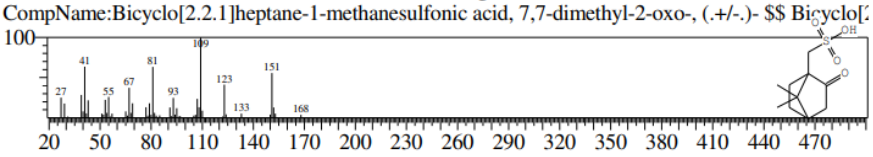

SI:71 Formula:C11H8O2 CAS:708-06-5 MolWeight:172 RetIndex:1754
CompName:1-Naphthalenecarboxaldehyde, 2-hydroxy- $$ 1-Naphthaldehyde, 2-hydroxy- $$ .beta.-H

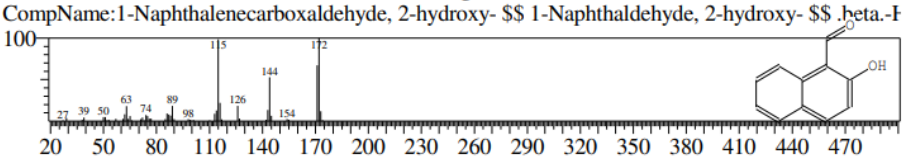

SI:65 Formula:C11H20 CAS:2958-76-1 MolWeight:152 RetIndex:1162
CompName:Naphthalene, decahydro-2-methyl- $$ Decahydro-2-methylnaphthalene $$ 2-Methyldeca

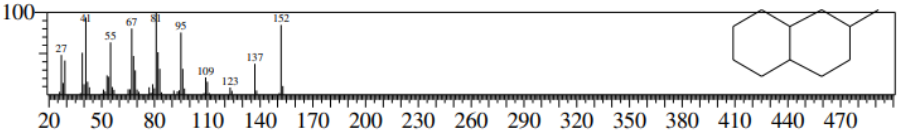

SI:70 Formula:C10H10O3 CAS:4676-39-5 MolWeight:178 RetIndex:1473
CompName:3,4-Methylenedioxyphenyl acetone $$ (3,4-(Methylenedioxy)phenyl)-2-propanone $$ 2-

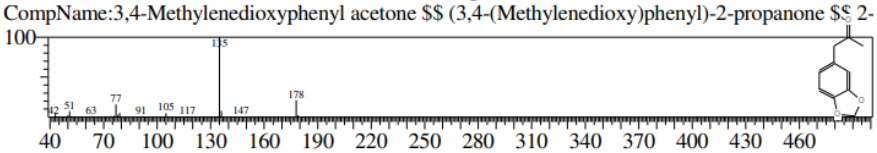

SI:82 Formula:C28H46O CAS:96391-64-9 MolWeight:398 RetIndex:2640
CompName:5,6-Dihydroergosterol $$ (22E)-Ergosta-7,22-dien-3-ol # $$

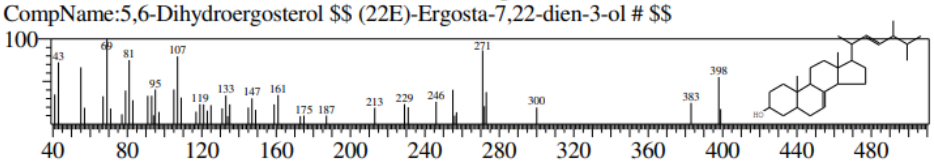

SI:91 Formula:C17H19NO3 CAS:94-62-2 MolWeight:285 RetIndex:2399
CompName:Piperine $$ Piperidine, 1-[5-(1,3-benzodioxol-5-yl)-1-oxo-2,4-pentadienyl]-, (E,E)- $$ P

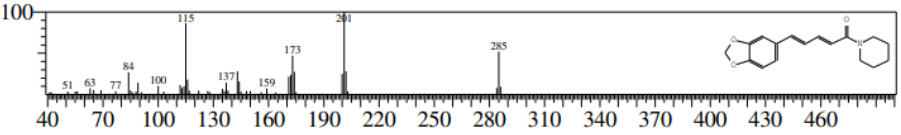

SI:52 Formula:C12H22O CAS:33956-49-9 MolWeight:182 RetIndex:1473
CompName:8,10-Dodecadien-1-ol, (E,E)- $$ Codlelure $$ E,E-8,10-Dodecadien-1-ol $$ (8E,10E)-8

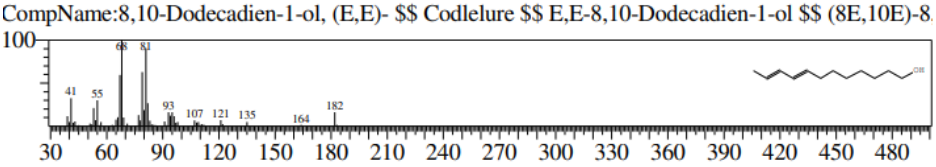

Figure S2. Mass spectral data of constituents identified by GC-MS in hexane extract

Mass Spectral Data of Constituents Identified by GC-MS in Ethyl acetate extract

SI:77 Formula:C6H14O6 CAS:69-65-8 MolWeight:182 RetIndex:1752
CompName:D-Mannitol $$ Mannitol, D- $$ Cordycepic acid $$ D-(-)-Mannitol $$ Diosmol $$ Isoto

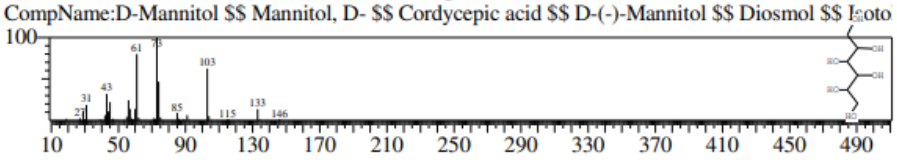

<< Target >>

SI:97 Formula:C9H14O CAS:78-59-1 MolWeight:138 RetIndex:1097
CompName:2-Cyclohexen-1-one, 3,5,5-trimethyl- $$ .alpha.-Isophoron $$ .alpha.-Isophorone $$ Iso

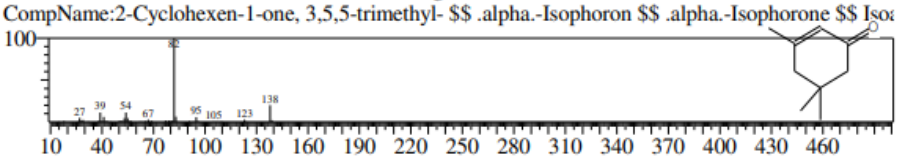

SI:86 Formula:C5H10O4 CAS:26446-35-5 MolWeight:134 RetIndex:1091
CompName:1,2,3-Propanetriol, monoacetate $$ Acetin, mono- $$ Acetin $$ Acetoglyceride $$ Acety

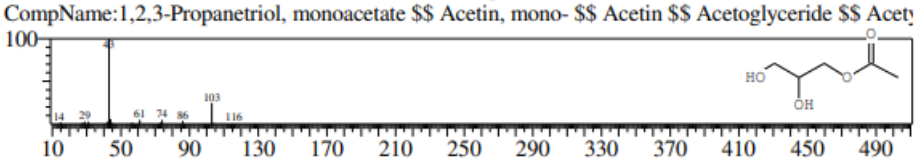

SI:95 Formula:C9H10O2 CAS:501-52-0 MolWeight:150 RetIndex:1349
CompName:Benzenepropanoic acid $$ Hydrocinnamic acid $$ .beta.-Phenylpropionic acid $$ Benze

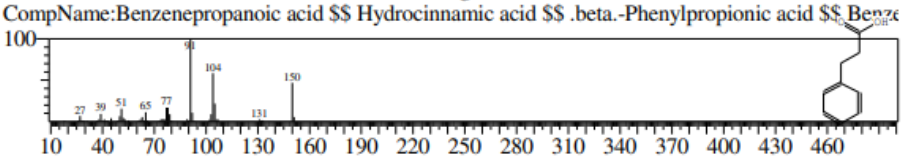

SI:93 Formula:C16H32 CAS:34303-81-6 MolWeight:224 RetIndex:1620
CompName:3-Hexadecene, (Z)- $$ (3Z)-3-Hexadecene # $$

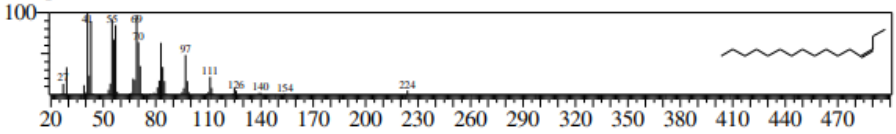

SI:94 Formula:C14H22O CAS:96-76-4 MolWeight:206 RetIndex:1555
CompName:Phenol, 2,4-bis(1,1-dimethylethyl)- $$ Phenol, 2,4-di-tert-butyl- $$ 2,4-Di-tert-butylpher

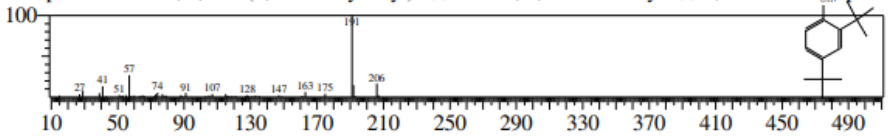

SI:90 Formula:C17H36O CAS:1454-85-9 MolWeight:256 RetIndex:1954
CompName:1-Heptadecanol $$ n-Heptadecanol $$ Heptadecyl alcohol $$ Heptadecan-1-ol $$ 1-Hy

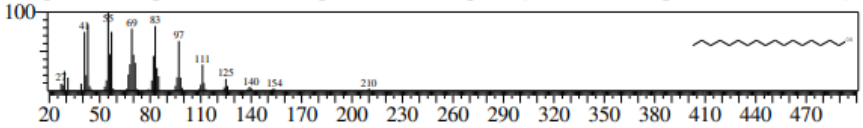

SI:80 Formula:C17H34 CAS:54290-12-9 MolWeight:238 RetIndex:1719
CompName:8-Heptadecene $$ (8E)-8-Heptadecene # $$

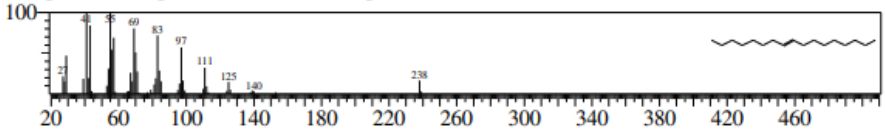

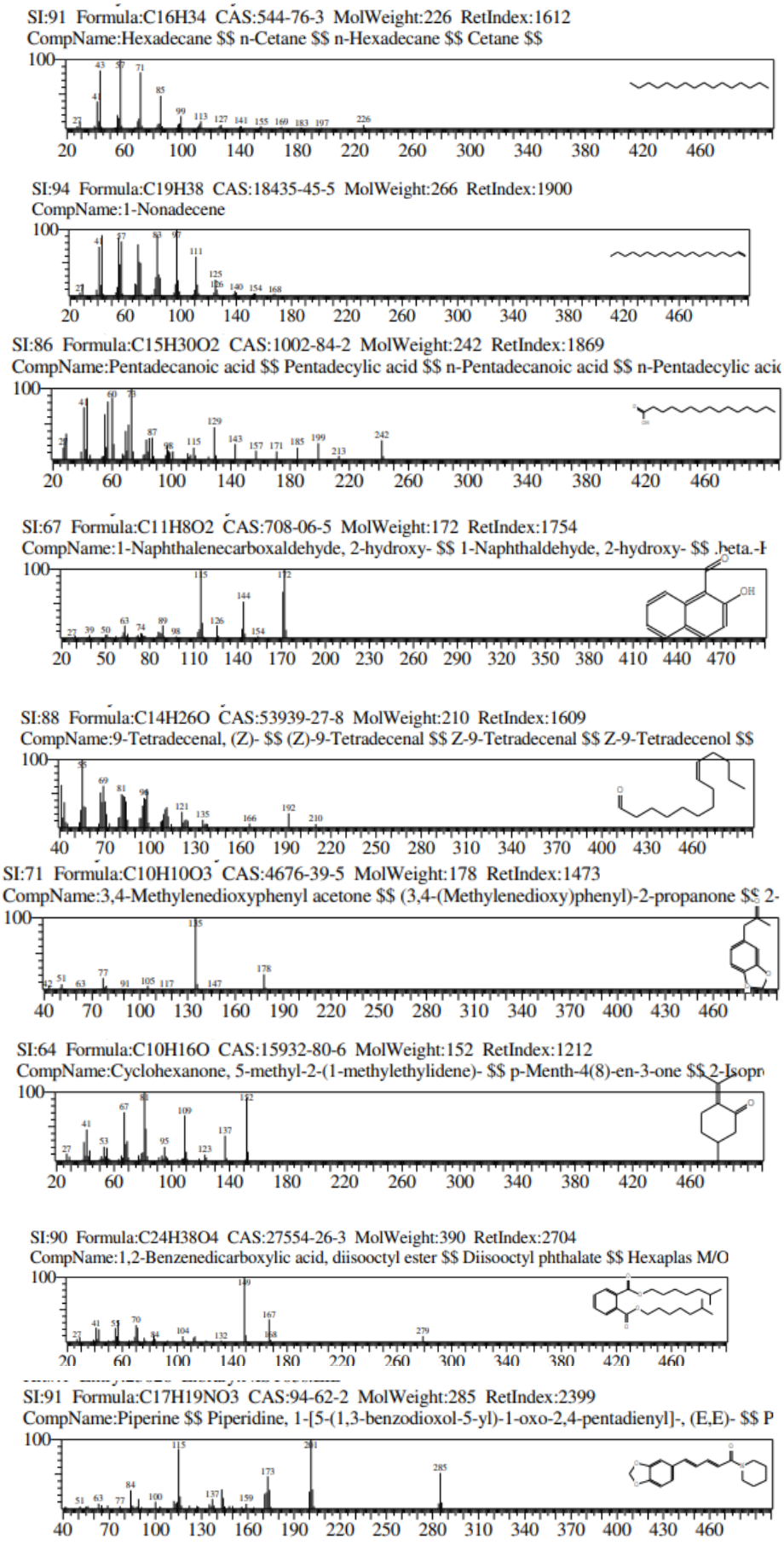

Figure S3. Mass spectral data of constituents identified by GC-MS in ethyl acetate extract

Mass Spectral Data of Constituents Identified by GC-MS in Methanol extract

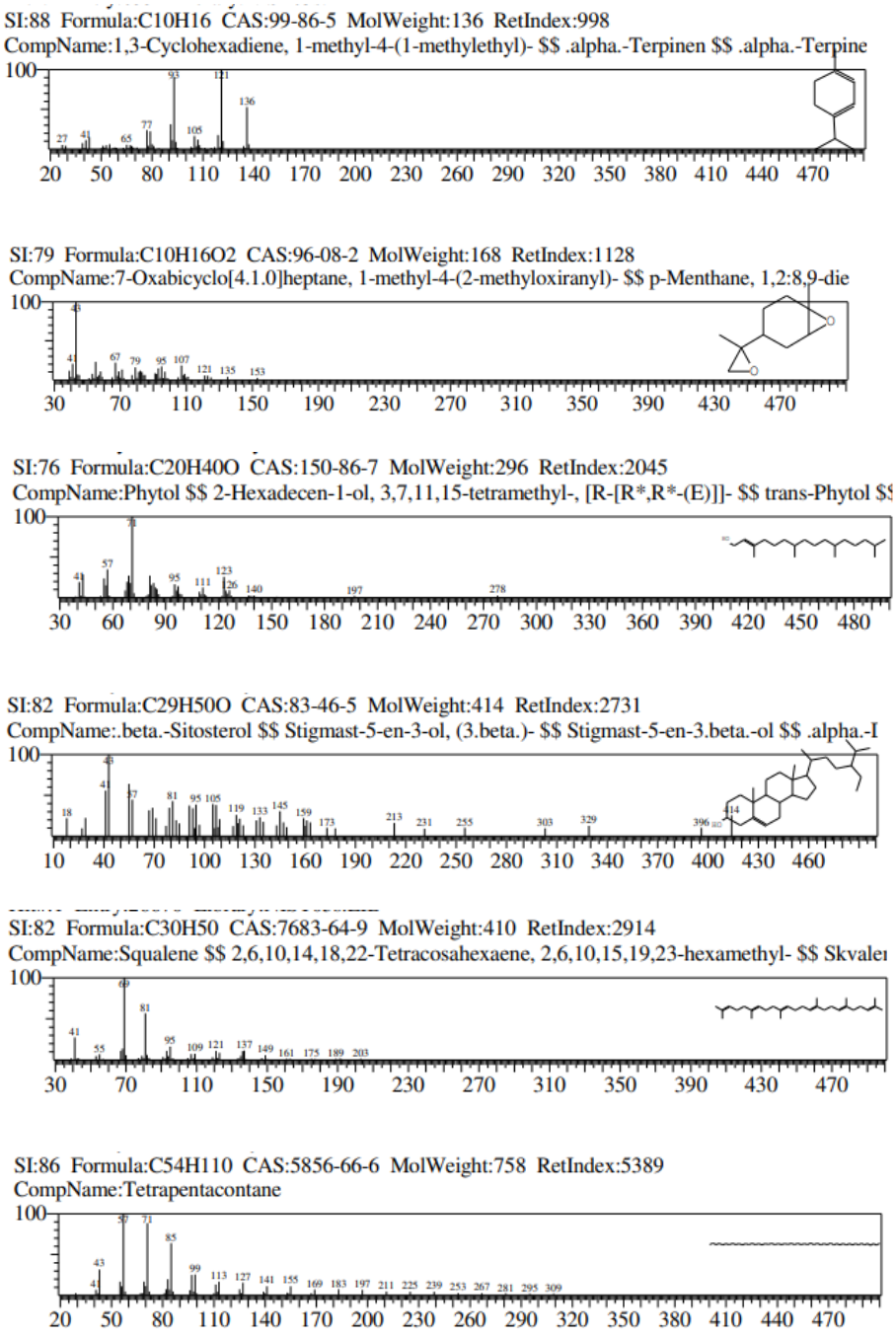

Figure S4. Mass spectral data of constituents identified by GC-MS in methanol extract